



(12)

Oversættelse af
europæisk patentskriftPatent- og
Varemærkestyrelsen

(51) Int.Cl.: **C 25 D 3/00 (2006.01)** **C 23 C 18/16 (2006.01)** **C 23 C 18/31 (2006.01)**
C 23 C 18/54 (2006.01) **C 25 D 15/00 (2006.01)** **C 25 D 15/02 (2006.01)**
C 25 D 21/14 (2006.01) **C 25 D 3/12 (2006.01)** **C 25 D 3/56 (2006.01)**

(45) Oversættelsen bekendtgjort den: **2022-01-10**

(80) Dato for Den Europæiske Patentmyndigheds
bekendtgørelse om meddelelse af patentet: **2021-09-29**

(86) Europæisk ansøgning nr.: **10794416.7**

(86) Europæisk indleveringsdag: **2010-06-29**

(87) Den europæiske ansøgnings publiceringsdag: **2012-05-09**

(86) International ansøgning nr.: **NZ2010000128**

(87) Internationalt publikationsnr.: **WO2011002311**

(30) Prioritet: **2009-06-29 NZ 57803809**

(84) Designerede stater: **AL AT BE BG CH CY CZ DE DK EE ES FI FR GB GR HR HU IE IS IT LI LT LU LV MC MK MT NL NO PL PT RO SE SI SK SM TR**

(73) Patenthaver: **Cirrus Materials Science Limited, 5b Target Court, Wairau Valley, Auckland, 0627, New Zealand**

(72) Opfinder: **GAO, Wei, 131 Porritt Avenue, Birkenhead, Auckland 0626, New Zealand**
CHEN, Weiwei, Room 309, New Blue Sky Centre, Auckland CBD, Auckland, New Zealand

(74) Fuldmægtig i Danmark: **Plougmann Vingtoft A/S, Strandvejen 70, 2900 Hellerup, Danmark**

(54) Benævnelse: **Fremgangsmåde til plettering eller belægning til fremstilling af metalkeramisk belægning på et substrat**

(56) Fremdragne publikationer:
EP-B1- 0 441 636
EP-B1- 1 020 542
WO-A1-2009/017266
CN-A- 101 397 657
DE-A1- 4 424 168
GB-A- 842 092
JP-A- H03 253 598
US-A- 3 617 363
US-A- 5 266 181
US-A- 5 935 403
US-B1- 6 183 908
None

DK/EP 2449154 T3

DESCRIPTION

FIELD OF INVENTION

[0001] The invention relates to an improved plating or coating method for producing a metal-ceramic composite coating on a substrate.

BACKGROUND

[0002] In electroplating sometimes referred to as electrodeposition, a conductive item to be metal plated which forms a cathode, and an anode, are immersed in an electrolyte containing one or more dissolved metal salts, and a battery or rectifier supplies direct current. In one method the anode is of the plating metal and metal molecules of the anode are oxidised and dissolved into the electrolyte and at the cathode the dissolved metal ions are reduced and plated onto the cathode/item. In another method the anode is not consumable and ions of the plating metal are provided in the electrolyte and must be periodically replenished.

[0003] Electroless plating or deposition is a non-galvanic plating or coating method in which a reducing agent, typically sodium hypophosphite, in aqueous solution reduces metal ions of the plating metal in solution from the anode, which deposit onto the cathode/item. Electroless nickel plating may be used to deposit a coating of nickel Ni-P or Ni-B onto a substrate which may be a metal or plastic substrate.

[0004] Electroless plating may also be used to form a metal-ceramic composite coating on a substrate, such as an Ni-P-TiO₂ coating for example. TiO₂ nanoparticles are added to the electroless plating solution and co-deposit on the substrate with the Ni-P in an Ni-P-TiO₂ matrix. The TiO₂ particles can tend to agglomerate together in solution and thus distribute non-uniformly on the substrate thus giving uneven properties to the coating, and with the objective of reducing this the solution is continuously stirred and/or a surfactant is added to assure good dispersion of the TiO₂ particles through the solution.

[0005] Ni-P- TiO₂ coatings may also be formed on a substrate or item by first forming a coating of Ni-P on the item by electroplating and then dipping the item into a TiO₂ sol to deposit TiO₂ on/in the coating by the sol-gel process.

[0006] Plating or coating of an item or surface is typically carried out to provide a desired property to a surface that otherwise lacks that property or to improve a property to a desired extent, such as abrasion or wear resistance, corrosion resistance, or a particular appearance, for example.

[0007] US 5,935,403 describes a magnetic thin film manufacturing method in which an object of treatment is electroplated in a plating bath so that a magnetic film is formed on the surface of the object of treatment. The plating bath contains two or more types of ions selected from a set consisting of Fe^{2+} ions, Ni^{2+} ions and Co^{2+} ions, and fine particles of an insulating material are dispersed in the plating bath. DE 44 24 168 describes metallic dispersion layers based on a metal matrix with embedded dispersoid non-metallic particles, in which the dispersoids are non-porous spherical oxide particles with a particle size of 0.01-5 microns, obtained by hydrolytic polycondensation of alkoxides. CN 101397657 relates to a method which adopts nano silicon dioxide sol and rare earth to strengthen a composite deposit comprising the following main steps: the preparation of a nano sol, the preparation of a plating solution and electroless composite plating, with the nano SiO_2 sol being directly added into the Ni-P chemical plating solution containing rare earth cerous sulfate to carry out plating. US 6,183,908 relates to a lithium ion nonaqueous secondary battery and a negative electrode material for a lithium ion nonaqueous secondary battery comprising a composite metal oxide containing an amorphous structure synthesized by a sol-gel method. JP 3-253598 describes fine particles dispersed and suspended in a plating liquid to coprecipitate the particles in a plating film. Before the particles are incorporated and suspended into the plating liquid, the particle surfaces are modified with a metal oxide or metal nitride by a sol-gel method. US 3,617,363 discloses processes for electroless metallizing workpieces to provide thereon a metal coating incorporating therein non-metallic wear-resisting particles.

SUMMARY OF INVENTION

[0008] The present invention is defined in and by the appended claims.

[0009] In broad terms in one aspect the invention comprises a method for producing a metal-ceramic composite coating on a substrate which includes adding a sol of a ceramic phase to the plating solution or electrolyte in an amount controlled to be sufficiently low that nanoparticles of the ceramic phase form directly onto or at the substrate,

wherein molecules of the ceramic phase exist in a net-structure in the sol,

wherein the sol is added in a ratio of 0.5 to 100 mls of sol per litre of the plating solution,

wherein the sol has a concentration of 20 to 250 grams of the ceramic phase per litre of the sol, and

wherein the ceramic phase is a single or mixed oxide or silicate of Ti, W, Si, Zr, Al, Y, Cr, Fe, Pb, Co, or a rare earth element,

such that the metal-ceramic coating forms on the substrate with a predominantly crystalline structure.

[0010] The invention also comprises a plating or coating method for producing a metal-ceramic composite coating on a substrate which includes adding the sol in an amount sufficiently low as to substantially avoid formation of nanoparticles of the ceramic phase, and/or agglomeration of particles of the ceramic phase, in the plating solution or electrolyte.

[0011] In certain embodiments the sol is added while carrying out the plating or coating and at a rate of sol addition controlled to be sufficiently low that nanoparticles of the ceramic phase form directly onto or at the substrate and/or that the metal-ceramic coating forms on the substrate with a predominantly crystalline structure and/or to substantially avoid formation of nanoparticles of the ceramic phase, and/or agglomeration of particles of the ceramic phase, in the plating solution or electrolyte. In these embodiments in which the sol is added to the plating solution at a controlled slow rate during plating, a sol having a sol concentration of 20 to 250 or more preferably 25 to 150 grams of the ceramic phase per litre of the sol may be added to the plating solution at a ratio of 0.5 to 100 ml of sol per litre of the plating solution, and the sol may be added at a rate in the range 0.001 to 0.1 or more preferably 0.005 to 0.02 mls per second.

[0012] In other embodiments the sol is added prior to carrying out the plating or coating. The sol is added in a low amount such that nanoparticles of the ceramic phase form directly onto or at the substrate and/or that the metal-ceramic coating forms on the substrate with a predominantly crystalline structure and/or to substantially avoid formation of nanoparticles of the ceramic phase, and/or agglomeration of particles of the ceramic phase, in the plating solution or electrolyte. In these embodiments in which the sol is added to the plating solution prior to plating, a sol having a sol concentration of 20 to 250 or more preferably 25 to 150 grams of the ceramic phase per litre of the sol may be added to the plating solution in a ratio of 0.5 to 100 or more preferably 1.25 to 25 mls of sol per litre of the plating solution.

[0013] In other embodiments sol may be added both prior to and during the plating or coating.

[0014] The ceramic phase is a single or mixed oxide, or silicate, of Ti, W, Si, Zr, Al, Y, Cr, Fe, Pb, Co, or a rare earth element.

[0015] In certain embodiments the coating, other than the ceramic phase comprises Ni, Ni-P, Ni-W-P, Ni-Cu-P, Ni-B, Cu, Ag, Au, Pd.

[0016] In certain embodiments the substrate is a metal substrate such as a mild steel, alloy steel, Mg, Al, Zn, Sn, Cu, Ti, Ni, Co, Mo, Pb or an alloy. In other embodiments the substrate is a non-metallic substrate such as a plastics or ceramic substrate.

[0017] The term 'sol' in this specification means a solution of the ceramic phase. It is believed that molecules of the ceramic phase such as molecules of TiO_2 exist in a net-structure in the sol, and during the plating process react at the surface with to form a crystalline metal - ceramic composite coating.

[0018] The plating process may be an electroless plating or coating process or alternatively be a galvanic plating process. Where the plating process is a galvanic plating process the plating current may be in the range 10 mA/cm² to 300 mA/cm² preferably 20 mA/cm² to 100 mA/cm².

[0019] In this specification plating and coating are used interchangeably.

[0020] The present disclosure also relates to an item or surface plated or coated by a process as described above.

[0021] The term "comprising" as used in this specification means "consisting at least in part of". When interpreting each statement in this specification that includes the term "comprising", features other than that or those prefaced by the term may also be present. Related terms such as "comprise" and "comprises" are to be interpreted in the same manner.

BRIEF DESCRIPTION OF THE FIGURES

[0022] In the subsequent description the following figures are referred to, in which:

Figure 1 is a schematic diagram of apparatus used in the experimental work subsequently described in some examples,

Figure 2 shows surface morphologies of (a) a conventional Ni-P coating, and novel Ni-P-TiO₂ composite coatings prepared at TiO₂ sol dripping rates of (b) 0.02 ml/s, (c) 0.007 ml/s and (d) 0.004 ml/s,

Figure 3 shows cross-sectional morphologies and elemental distributions of (a1, a2) a conventional Ni-P coating, and novel Ni-P-TiO₂ composite coatings prepared at TiO₂ sol dripping rates of (b1, b2) 0.02ml/s, (c1, c2) 0.007ml/s, and (d1, d2) 0.004ml/s,

Figure 4 shows XRD spectra of Ni-P-TiO₂ composite coatings prepared at different sol dripping rates of (a) 0.004ml/s, (b) 0.007ml/s and (c) 0.02ml/s, and of (d) a conventional Ni-P coating,

Figure 5 shows microhardness of Ni-P-TiO₂ composite coatings prepared at different sol dripping rates,

Figure 6 shows wear track images for (a) a conventional Ni-P coating, and novel Ni-P-TiO₂ composite coatings prepared with the TiO₂ sol dripping rates of (b) 0.02ml/s, (c) 0.007ml/s and (d) 0.004ml/s,

Figure 7 shows surface morphologies of (a) a conventional Ni-P coating, and novel Ni-P-TiO₂ composite coatings prepared at different concentrations of TiO₂ sol of (b) 30 ml/L, (c) 60 ml/L, (d) 90 ml/L, (e) 120 ml/L, (f) 150 ml/L, and (g) 170 ml/L,

Figure 8 shows XRD spectra of (a) a conventional Ni-P coating, and novel Ni-P-TiO₂ composite

coatings prepared at TiO_2 sol concentrations of: (b) 30 ml/L, (c) 60 ml/L, (d) 90ml/L, (e) 120 ml/L, (f) 150 ml/L, and (g) 170 ml/L,

Figure 9 shows microhardness of the novel Ni-P- TiO_2 coatings prepared at different concentrations of TiO_2 sol,

Figure 10 shows wear tracks of (a) a conventional Ni-P coating, and novel Ni-P- TiO_2 coatings prepared at TiO_2 sol concentrations of (b) 30 ml/L, (c) 60 ml/L, (d) 90 ml/L, (e) 120 ml/L, (f) 150 ml/L, and (g) 170 ml/L,

Figure 11 shows surface morphologies of (a) a conventional electroplating Ni coating, and Ni- TiO_2 composite coatings prepared at different concentrations of TiO_2 sol: (b) 1.25 ml/L, (c) 2.5 ml/L, (d) 7.5 ml/L, (e) 12.5 ml/L, (f) 50 ml/L.

Figure 12 shows micro-hardness results of Ni- TiO_2 composite coatings prepared at different concentrations of TiO_2 sol,

Figure 13 shows wear volume loss of Ni- TiO_2 composite coatings prepared at different concentrations of TiO_2 sol,

Figure 14 shows the surface morphologies of Ni- TiO_2 composite coatings prepared at different plating currents: (a) 10 mA/cm², (a) 50 mA/cm², (a) 100 mA/cm².

Figure 15 shows micro-hardness results of Ni- TiO_2 composite coatings prepared at different plating currents,

Figure 16 shows wear volume loss of Ni- TiO_2 composite coatings prepared at different currents,

Figure 17 shows the surface morphologies of ultra-black surfaces of Ni-P- TiO_2 composite coatings prepared with dripping rates of TiO_2 sol of (a) 0.007 ml/s and (b) 0.004 ml/s.

Figure 18 shows the cross-sectional morphologies of ultra-black surfaces of Ni-P- TiO_2 composite coatings prepared with dripping rates of TiO_2 sol of (a) 0.007 ml/s and (b) 0.004 ml/s.

Figure 19 shows the reflectance of ultra-black surfaces of Ni-P- TiO_2 composite coatings prepared with dripping rates of TiO_2 sol of 0.007 and 0.004ml/s,

Figure 20 shows the surface morphologies of ultra-black surfaces of Ni-P- TiO_2 composite coatings prepared with concentrations of TiO_2 sol at (a)50 ml/L, (b)90 ml/L, (c)120 ml/L and (b)150 ml/L.

Figure 21 shows the cross-sectional morphologies of ultra-black surfaces of Ni-P- TiO_2 composite coatings prepared with concentrations of TiO_2 sol at (a) 50 ml/L, (b)90 ml/L, (c)120

ml/L and (b) 150 ml/L.

Figure 22 shows the reflectance of ultra-black surfaces of Ni-P-TiO₂ composite coatings prepared with concentrations of TiO₂ sol at 50, 90, 120 and 150 ml/L.

Figure 23 shows the surface morphologies of (a) a conventional electroless plated Ni-P coating, (b) a conventional Ni-P-ZrO₂ composite coating, and (c) a novel Ni-P-ZrO₂ composite coating with the sol concentration of 120 ml/L.

Figure 24 shows the XRD spectra of (a) a conventional electroless plated Ni-P coating, (b) a conventional Ni-P-ZrO₂ composite coating, and (c) a novel Ni-P-ZrO₂ composite coating with the sol concentration of 120 ml/L.

Figure 25 shows the microhardness of (a) a conventional electroless plated Ni-P coating, (b) a conventional Ni-P-ZrO₂ composite coating, and (c) a novel Ni-P-ZrO₂ composite coating with the sol concentration of 120 ml/L.

Figure 26 shows surface second-electron morphologies of (a) a conventional Ni-TiO₂ composite coating, and (b) a novel sol-enhanced Ni-TiO₂ composite coating. The insets in (a) and (b) are locally magnified backscattered electron images.

Figure 27 shows the variation of microhardness as a function of the annealing temperature for a conventional Ni-TiO₂ composite coating and a novel sol-enhanced Ni-TiO₂ composite coating.

Figure 29 shows wear tracks on (a) a conventional Au coating, and (b) a novel sol-enhanced Au coating.

Figure 30 shows wear tracks on (a) a conventional Au coating, and (b) a novel sol-enhanced Au coating.

Figure 31 shows the effect of Al₂O₃ sol concentration on the microhardness of coatings.

DETAILED DESCRIPTION OF EMBODIMENTS

[0023] The invention comprises a method for producing a metal-ceramic composite coating on a substrate which includes adding a sol of a ceramic phase to the plating solution or electrolyte.

[0024] The sol may have a concentration such that the sol is transparent (particles of the ceramic phase are not visibly present in the sol), and may in certain embodiments have a concentration of the ceramic phase of between about 20 to about 100 g/litre.

[0025] Where the sol of the ceramic phase is added to the solution or electrolyte during the plating process it may be added throughout the plating or coating process, or in certain embodiments for less than all of the duration of the plating process but at least 80% or at least 70% or at least 60% or at least 50% of the duration of the plating process. Optionally an amount of the sol may also be added to the solution or electrolyte prior to the commencement of plating or coating.

[0026] The sol may be added to the plating solution at the required slow rate by dripping or spraying the sol into the plating solution or by any other technique by which the sol can be added at the required slow rate.

[0027] It is believed in relation to some embodiments that if the ceramic phase is added as a sol during plating and at a sufficiently slow rate and low concentration, molecules of the ceramic phase from the sol form nanoparticles in situ on or at the surface of the substrate, and that a metal-ceramic composite coating having a largely crystalline rather than an amorphous structure is formed.

[0028] The ceramic phase is a single or mixed oxide, or silicate, of Ti, W, Si, Zr, Al, Y, Cr, Fe, Pb, Co, or a rare earth element.

[0029] In certain embodiments the substrate is a metal substrate such as mild steel, alloy steel, Mg, Al, Zn, Sn, Cu, Ti, Ni, Co, Mo, Pb or an alloy. In other embodiments the substrate is a non-metallic substrate such as a plastics and ceramic substrate.

[0030] The plating or coating may be carried out to provide improved abrasion or wear resistance or corrosion resistance to an item or surface, to provide an electrically conductive coating on a surface or item, or to alter optical properties, for decorative purposes, for example.

[0031] By the process of the invention we have been able to achieve Ni-P- TiO₂ coatings having microhardness of about 1025HV. In a conventional electroplating process in which TiO₂ nanoparticles are added to the plating solution before the commencement of the plating and not in a sol, hardness of the order of 670-800HV is typically achieved.

[0032] In another particular embodiment where the substrate is mild carbon steel, the substrate plated or coated by the process of the invention has very low light reflection i.e. is ultra-black.

[0033] The plating process may be an electroless plating or coating process, in which the anode comprises the plating metal, the cathode the item to be plated or coated, and the ceramic phase is added as a sol to the solution comprising a reducing agent such as sodium hypophosphite, sodium borohydride, formaldehyde, dextrose, rochelle salts, glyoxal, hydrazine sulfate.

[0034] The plating process may alternatively be a galvanic plating process in which the anode comprises the plating metal, or ions of the plating metal are provided in the electrolyte, the cathode comprises the item to be plated, and the ceramic phase is added to the electrolyte as a sol.

EXAMPLES

[0035] The following description of experimental work further illustrates the invention by way of example:

Example 1 - Ni-P-TiO₂ composite coating on Mg alloy by electroless plating, at different sol rates

[0036] A transparent TiO₂ sol was prepared in the following way: 8.68 ml of titanium butoxide (0.04 g/ml) was dissolved in a mixture solution of 35 ml of ethanol and 2.82 ml diethanolamine. After magnetic stirring for 2 hours, the obtained solution was hydrolyzed by the addition of a mixture of 0.45 ml deionized water and 4.5 ml ethanol dropwise under magnetic stirring. After stirring for 2 hours, the TiO₂ sol was kept in a brown glass bottle to age for 24 hours at room temperature.

[0037] The transparent TiO₂ sol was added into 150 ml of a conventional Ni-P electroless plating (EP) solution by dripping at a controlled rate during plating (1 drop = 0.002 ml approx). During plating the solution was continuously stirred by magnetic stirring at the speed of ~200r/min. The solution temperature was kept at 80-90°C and the plating time was -90 min. Figure 1 shows the experimental apparatus used. In Figure 1 the following reference numerals indicate the following parts:

1. 1. Separatory funnel
2. 2. TiO₂ sol outlet
3. 3. Lids
4. 4. Erlenmeyer
5. 5. Beaker
6. 6. Water
7. 7. Electroless plating solution
8. 8. Samples
9. 9. Bracket
10. 10. Magnetic stirrer
11. 11. Siderocradle
12. 12. Funnel stand

[0038] The plating process was repeated at different sol dripping rates and sol concentrations.

[0039] On analysis the coatings were found to be mainly crystalline, and to have micro-hardness up to $1025 \text{ HV}_{0.2}$, compared to $\sim 590 \text{ HV}_{0.2}$ for conventional Ni-P coatings and $\sim 700 \text{ HV}_{0.2}$ for conventional Ni-P-TiO₂ composite coatings. The width of the wear tracks of the coating was reduced to about 160 μm in some cases, compared to the corresponding width for the conventional composite coating of about 500 μm .

[0040] Figure 2 shows surface morphologies of the Ni-P-TiO₂ composite coatings produced at sol dripping rates of 0.004, 0.007, 0.02ml/s, at a concentration of TiO₂ sol 120 ml/L.

[0041] Referring to Figure 2a the conventional EP Ni-P coating has a typical "cauliflower-like" structure with some pores caused by formation of H₂ in the EP process as shown by the arrows.

[0042] With TiO₂ sol dripped into the EP Ni-P solution at a rate of 0.02ml/s, the "cauliflower" structure became smaller - see Figure 2b Clusters of micro-Ni crystals formed in the interfaces, indicating that the TiO₂ sol addition promoted the nucleation of Ni crystals and prevented the growth of Ni crystals.

[0043] Figure 2c shows the coating produced at a sol dripping rate of 0.007ml/s. It was compact and smooth coating of Figure 2a. Well-dispersed white nano-particles were distributed on the surface as shown by the arrows on the right top inset in Figure 2c. It is believed that these particles are TiO₂ nano-particles.

[0044] At a TiO₂ sol dripping rate of 0.004ml/s, the coating was also compact and smooth - see Figure 2d. Loose TiO₂ particles congregated in the interfaces between Ni crystals as shown by the arrows in the Figure 2d.

[0045] Figure 3 shows cross-sectional morphologies and elemental distributions of an Ni-P coating, and of Ni-P-TiO₂ composite coatings prepared at the different dripping rates of TiO₂ sol.

[0046] The conventional Ni-P coating is compact with a thickness of -25 μm - see Figure 3a1, and good adhesion to the Mg substrate. The Ni and P elements have homogeneous distributions along the coating - see Figure 3a2.

[0047] Figures 3b1 and 3b2 show the microstructure and elemental distributions of the Ni-P-TiO₂ composite coating prepared with a sol dripping rate of 0.02ml/s. The coating was thinner than the Ni-P coating. The thickness further decreased, from about 23 μm to around 20 μm at a sol dripping rate of 0.007ml/s - Figures 3c1 and 3c1, and to 18 μm at a dripping rate of 0.004ml/s - see Figure 3d1.

[0048] Figures 4a-c show the XRD spectra for the Ni-P-TiO₂ composite coatings prepared at the different dripping rates, and Figure 4d for the Ni-P coating. The conventional EP medium P content coating possesses a typical semi-crystalline structure, i.e. mixture of amorphous phase and crystallized phase, while the Ni-P-TiO₂ composite coatings possess fully crystalline phase structures.

[0049] The composite coatings produced by the process of the invention possess hardness up to about 1025 HV₂₀₀, compared to about 710 HV₂₀₀ for composite coatings prepared by powder methods and about 570HV₂₀₀ for conventional Ni-P coatings. Figure 5 shows the microhardness of the Ni-P-TiO₂ composite coatings prepared at sol dripping rates of from 0.004ml/s to 0.02ml/s. Greatest hardness was obtained at the dripping rate of 0.007ml/s.

[0050] In Figure 6a the width of wear track of the conventional Ni-P coating was about 440 µm. Many deep plough lines are observed. In contrast, the novel Ni-P-TiO₂ composite coatings possessed better wear resistance as seen from Figures 6b, c and d. The wear track of the composite coatings had a narrower width of about 380 µm at 0.02ml/s, 160 µm at 0.007ml/s, and 340 µm at 0.004ml/s.

[0051] The novel composite coatings also had very few plough lines compared with the conventional Ni-P coatings.

Example 2 - Ni-P TiO₂ composite coatings on Mg by electroless plating, at different sol concentrations

[0052] The effect of TiO₂ concentration in the sol was also studied. Ni-P-TiO₂ composite coatings were prepared as described in Example 1 but with a constant sol dripping rate of 0.007ml/s and at sol concentrations of TiO₂ sol at 30, 60, 90, 120, 150 and 170 ml/L (1.2, 2.4, 3.6, 4.8, 6.0, 6.8 g/L).

[0053] Figure 7 shows surface morphologies of a conventional Ni-P coating and the novel Ni-P-TiO₂ composite coatings prepared at different TiO₂ sol concentrations.

[0054] Figure 7a shows the typical "cauliflower"-like structure of the conventional Ni-P coating with some pores on the surface due to the formation of H₂ in the EP process as shown by the arrows.

[0055] Figures 7b and 7c show the surface morphologies of the composite coatings with TiO₂ sol dripped into the EP solution at concentrations of 30 ml/L and 60 ml/L, respectively. No white TiO₂ particles were observed in the EP solution during the process. Many micro-sized Ni crystallites formed and congregated on the big Ni grains or in the low-lying interfaces between

Ni grains - see Figure 7b. At a sol concentration of 60 ml/L, many well-dispersed and micro-sized Ni crystallites formed on the surface with no congregation - see Figure 7c, and the Ni crystallites became smaller with a smoother surface. White TiO_2 particles were formed in the EP solution as the sol concentration increased.

[0056] Figure 7d shows the surface morphology of the coating produced at a sol concentration of 90 ml/L. Micro-sized Ni crystallites are smaller with good dispersion. Large-scale Ni crystals were observed with many small and well-dispersed Ni crystallites on them as shown by the arrows in Figure 7d. At a sol concentration of 120 ml/L, micro-sized Ni crystals almost disappeared - see Figure 7e, and nano-sized TiO_2 particles were observed on the surface with good dispersion as shown by the arrows in the inset of Figure 7e.

[0057] Figure 8 shows XRD spectra of the conventional Ni-P coating and the novel Ni-P- TiO_2 composite coatings at the different concentrations of TiO_2 sol. The conventional EP Ni-P coating has a typical semi-crystallized structure, i.e. a mixture of amorphous and crystalline phases - see Figure 5a, while the novel Ni-P- TiO_2 composite coatings have different phase structures with better crystallinity at the lower concentrations of TiO_2 sol as shown in Figures 8b, 8c, 8d and 8e. The coatings have a semi-crystalline structure at higher sol concentrations of 150 and 170 ml/L - see Figures 8f and 8g.

[0058] The effect of sol concentration on the microhardness of the composite coatings is shown in Figure 9. At relatively low TiO_2 sol concentrations of 30 - 60 ml/L, the microhardness was about 700 HV_{200} . No white TiO_2 particles were observed. At sol concentrations of from 60 to 120 ml/L white TiO_2 particles were observed in the EP solution, and the microhardness increased to a peak of about 1025 HV_{200} .

[0059] Images of wear tracks on the conventional Ni-P coating and the novel Ni-P- TiO_2 composite produced at different concentrations of TiO_2 sol are shown in Figure 10.

[0060] At sol concentrations of 30-60 ml/L the wear tracks became discontinuous as shown in Figures 10b and 10c, and almost no plough lines are observed. At sol concentrations of 90-120ml/L the tracks became narrower (but more continuous) - the width of tracks decreased from $\sim 240 \text{ } \mu\text{m}$ to $\sim 160 \text{ } \mu\text{m}$. Figures 10d and 10e show the wear tracks on coatings produced at sol concentrations of 150 and 170 ml/L.

[0061] We observed that when the sol was dripped into the EP solution it fast diluted under stirring. The solution was kept transparent and no white particles could be seen by the naked eye, implying that the TiO_2 particles are very small. The TiO_2 nano-particles have no opportunity to agglomerate together to form clusters. Therefore nano-sized TiO_2 particles are deposited together with Ni, forming a metal/nano-oxide composite coating. The nano-particle dispersion also contributes to the improved hardness and wear resistance.

Example 3 - Ni-TiO₂ coating on mild steel by electroplating, at different sol concentrations

[0062] A Ni-TiO₂ electroplating coating was formed on carbon steel by adding a TiO₂ sol prepared as described in example 1 into a traditional Ni electroplating solution at the commencement of electroplating. The bath composition and electroplating parameters are listed in the table below. 12.5ml/l of transparent TiO₂ sol solution prepared as described in example 1 was added to the electroplating solution, and then Ni-TiO₂ composite coatings were formed on carbon steels with a current of 50 mA/cm². Ni and Ni-TiO₂ coatings were prepared without sol addition for comparison.

[0063] The Ni-TiO₂ coating was prepared with a concentration of TiO₂ nano-particles (diameter < 25 nm) of 10 g/L.

Bath composition/parameters	Quantity
NiSO ₄ •6H ₂ O	300 g/L
NiCl ₂ •6H ₂ O	45 g/L
H ₃ BO ₃	40 g/L
TiO ₂ sol	12.5 mL/L
pH	3.8
Temperature	Room temperature (20°C)
Current <i>i</i>	50 mA/cm ²
Time	10 min

[0064] The Ni-TiO₂ composite coating formed had a micro-hardness of 428 HV₁₀₀, compared to 356 HV₁₀₀ for the Ni-TiO₂ composite coating formed conventionally and 321 HV₁₀₀ for the Ni coating.

[0065] Coatings were prepared at TiO₂ sol concentrations of 0, 1.25, 2.5, 7.5, 12.5 and 50ml/L (0, 0.05, 0.0625, 0.3, 0.5, 2 g/L).

[0066] Figure 11 shows surface morphologies of the Ni-TiO₂ composite coatings prepared at sol concentrations of 0, 1.25, 2.5, 7.5, 12.5 and 50ml/L.

[0067] Figure 12 shows microhardness of the Ni-TiO₂ composite coatings prepared at sol concentrations of 0, 1.25, 2.5, 7.5, 12.5 and 50ml/L. The microhardness of the Ni coating was nearly 320HV₁₀₀. The Ni-TiO₂ composite coatings had increased microhardness, up to

428HV₁₀₀, at the sol concentrations of 1.25ml/L to 12.5ml/L.

[0068] Referring to Figure 13 the Ni coating had the worst wear volume loss at about 8×10^{-3} mm³. The Ni-TiO₂ composite coatings had better wear resistance.

Example 4 - Ni-TiO₂ coating on mild steel by electroplating, at different currents

[0069] Coatings were prepared as in Example 3 but at different plating currents. Figure 14 shows the surface morphologies of Ni-TiO₂ composite coatings prepared with 12.5ml/L TiO₂ sol addition at currents of 10, 50, 100mA/cm².

[0070] Figure 15 shows the microhardness of Ni-TiO₂ composite coatings prepared with 12.5ml/L TiO₂ sol addition at currents of 10, 50, 100mA/cm². At 10mA/cm² the coating had a microhardness of about 300HV₁₀₀, the microhardness increased to 428HV₁₀₀ at 50mA/cm², and the microhardness was about 380HV₁₀₀ at current of 100mA/cm².

[0071] Figure 16 shows wear volume loss of the Ni-TiO₂ composite coatings. The coating had best wear resistance at 50mA/cm², with a wear volume loss of about 0.004mm³.

Example 5 - Ultra-black Ni-P-TiO₂ composite coating on carbon steel, by electroless plating

[0072] An Ni-P-TiO₂ electroless coating with ultra-black surface was formed on carbon steel through adding TiO₂ sol prepared as in example 1 into a conventional Ni electroless solution at a controlled rate. When 90ml/L (3.6 g/L) transparent TiO₂ solution was added at a rate of 0.007ml/s to a plating solution of 150 ml, a Ni-P-TiO₂ electroless coating with an ultra-black surface with the lowest reflectance at 0.1-0.5% of visible light was formed.

[0073] Figure 17 shows the surface morphologies of Ni-P-TiO₂ composite coatings prepared at different sol addition rates of 0.007 and 0.004ml/s.

[0074] Figure 18 shows the cross-sectional morphologies of Ni-P-TiO₂ composite coatings prepared at different sol addition rates.

[0075] Figure 19 shows the reflectance of the ultra-black surfaces of Ni-P-TiO₂ composite coatings prepared at different sol addition rates, in the range of visible light. Lower reflectance was obtained when the TiO₂ sol was added at 0.007ml/s.

[0076] Figure 20 shows the surface morphologies of Ni-P-TiO₂ composite coatings prepared at different sol concentrations of 50, 90, 120 and 150 ml/L.

[0077] Figure 21 shows the cross-sectional morphologies of Ni-P-TiO₂ composite coatings prepared at different sol concentrations.

[0078] Figure 22 shows the reflectance of ultra-black surfaces of Ni-P-TiO₂ composite coatings in the range of visible light prepared at different sol concentrations.

Example 6 - Cu-TiO₂ coatings on carbon steel, by electroplating

[0079] A small amount of TiO₂ sol prepared as in example 1 was added into a conventional electroplating Cu solution, leading to the *in situ* synthesis of Cu-TiO₂ composite coatings. This novel Cu-TiO₂ composite coating had a micro-hardness of 210 HV, compared to 150 HV of the traditional Cu coating, showing 40% increase.

Example 7 - Ni-P-ZrO₂ composite coating on Mg alloy, by electroless plating

[0080] A transparent ZrO₂ sol was prepared in the following way: 45 ml of zirconium propoxide was dissolved in a mixture solution of 124 ml of ethanol and 11.3 ml diethanolamine. After magnetic stirring for 2 hours, the obtained solution was hydrolyzed by the addition of a mixture of 1.84 ml deionized water and 16.2 ml ethanol dropwise under magnetic stirring. After stirring for 2 hours, the ZrO₂ sol was kept in a brown glass bottle to age for 24 hours at room temperature. The transparent ZrO₂ sol was added into a conventional Ni-P electroless plating (EP) solution by dripping at a controlled rate during plating (1 drop = 0.002 ml approx). During plating the solution was continuously stirred by magnetic stirring at the speed of ~200 r/min. The solution temperature was kept at 80-90°C and the plating time was ~90 min.

[0081] Figure 23 shows surface morphologies of the Ni-P-ZrO₂ composite coatings produced at sol dripping rates of 0.007ml/s, at a concentration of ZrO₂ sol 120 ml/L.

[0082] Figure 24 show the XRD spectra of the Ni-P-ZrO₂ composite coatings produced at sol dripping rates of 0.007ml/s, at a concentration of ZrO₂ sol 120 ml/L.

[0083] The traditional electroless plated Ni-P and Ni-P-ZrO₂ coatings possessed a typical semi-crystallization, i.e. the mixture of crystallization and amorphous state, as shown in Figure 24 a and b. In contrast, the Ni-P-ZrO₂ composite coating had a fully crystallized state as shown in Figure 24c.

[0084] Figure 25 shows the mechanical properties of the Ni-P-ZrO₂ composite coatings produced at sol dripping rates of 0.007 ml/s, at a concentration of ZrO₂ sol 120 ml/L.

[0085] The microhardness of the Ni-P-ZrO₂ composite coating was increased to 1045 HV₂₀₀ compared to 590 HV₂₀₀ of the conventional Ni-P coating and 759 HV₂₀₀ of the conventional Ni-P-ZrO₂ composite coating.

Example 8 - Ni-TiO₂ composite coatings on mild carbon steel

[0086] A Ni-TiO₂ electroplating coating was deposited on mild carbon steel by adding a TiO₂ sol prepared as described in example 1 into a traditional Ni electroplating solution during electroplating and at a low and controlled rate. 12.5 ml/l of transparent TiO₂ sol solution was added into the electroplating solution, and then Ni-TiO₂ composite coatings were formed on carbon steels with a current of 50 mA/cm². Ni-TiO₂ coatings were prepared with solid TiO₂ nano-particles (diameter < 25 nm) of 10 g/L for comparison.

[0087] Figure 26 shows surface second-electron morphologies of: (a) a conventional Ni-TiO₂ composite coating, and (b) the sol-enhanced Ni-TiO₂ composite coating. The insets in (a) and (b) are locally magnified backscattered electron images. The traditional Ni-TiO₂ coating exhibited a quite rough and uneven surface (Figure 26a). Large spherical Ni nodules with the size of ~4 µm were clearly seen, on which there were many superfine Ni nodules (~300 nm) as shown in the inset in Figure 1a. Large clusters of TiO₂ nano-particles (~400 nm) were incorporated in the Ni nodules, as pointed by the arrows in the inset (BSE image). In contrast, the sol-enhanced Ni-TiO₂ composite coating had a much smoother surface (Figure 26b). Two shapes of Ni nodules, i.e. spherical and pyramid-like, were displayed on the surface. The pyramid-like Ni nodules with ~1.5 µm size were relatively uniformly distributed in the spherical Ni nodules. It can be clearly seen from the inset in Figure 1b that the size of the spherical Ni nodules was quite small, ~200 nm.

[0088] Figure 27 shows the variation of microhardness as a function of the annealing temperature: ■-conventional Ni-TiO₂ composite coating; ●- sol-enhanced Ni-TiO₂ composite coating. The as-deposited sol-enhanced coating possessed a high microhardness of ~407 HV₅₀ compared to ~280 HV₅₀ of the conventional coating. The microhardness of the conventional coating was ~280 HV₅₀ after low-temperature annealing (up to 150°C), followed by a relatively steady decline to ~180 HV₅₀ when the coating was annealed at 400°C for 90 min. In contrast, for the sol-enhanced coating, the high microhardness (~407 HV₅₀) can be stabilized up to 250°C.

[0089] Figure 28 shows the engineering stress-strain curves for (A) the conventional and (B)

the sol-enhanced Ni-TiO₂ composites tested at a strain rate of $1 \times 10^{-4} \text{ s}^{-1}$. The sol-enhanced composite shows a significantly increased tensile strength of ~1050 MPa with ~1.4% strain, compared to ~600 MPa and ~0.8% strain of the traditional composite.

Example 9 - Au-TiO₂ composite coating on Ni-coated brass

[0090] A small amount of TiO₂ sol prepared as described in example 1 was added into the conventional 1 electroplating Au solution, leading to the synthesis of Au-TiO₂ composite coatings. The microhardness and wear resistance were greatly improved as summarised in the table below.

Microhardness of traditional Au and sol-enhanced Au-TiO₂ composite coatings

	Group I		Group II	
	Condition: 10 mA/cm ² , 6.5 min		Condition: 50 mA/cm ² , 2.5 min	
	Microhardness (HV ₁₀)	Wear volume loss ($\times 10^{-3} \text{ mm}^3$)	Microhardness (HV ₁₀)	Wear volume loss ($\times 10^{-3} \text{ mm}^3$)
Conventional Au	242 ± 6	1.58 ± 0.02	248 ± 4	1.62 ± 0.02
Novel sol-enhanced Au	269 ± 7	1.43 ± 0.02	293 ± 10	0.82 ± 0.03
Improvement	11%	10.5% or reduced to 90%	18%	98% or reduced to 50.6%

[0091] Figure 29 shows the wear tracks on (a) the conventional Au coating, and (b) the sol-enhanced Au coating. The electroplating was carried out with a current density of 10 mA/cm² for 6.5 min. The wear volume loss was measured and calculated from the width of the wear track. It was found that the wear volume loss of the conventional Au coating was ~ $1.58 \times 10^{-3} \text{ mm}^3$, compared to ~ $1.43 \times 10^{-3} \text{ mm}^3$ of the sol-enhanced Au coating.

[0092] Figure 30 shows the wear tracks on (a) the conventional Au coating, and (b) the sol-enhanced Au coating. The electroplating was carried out with a current density of 50 mA/cm² for 2.5 min. It was calculated that the wear volume loss of the conventional Au coating was ~ $1.62 \times 10^{-3} \text{ mm}^3$, compared to ~ $0.82 \times 10^{-3} \text{ mm}^3$ of the sol-enhanced Au coating, indicating that the wear resistance of sol-enhanced coatings was significantly improved.

Example 10 - Cu-ZrO₂ composite coating on carbon steel

[0093] ZrO_2 sol prepared as described in example 7 was added into a conventional electroplating Cu solution, leading to the synthesis of Cu- ZrO_2 composite coatings. Cu and Cu- ZrO_2 (solid-particle mixing) coatings were also prepared with a concentration of ZrO_2 nanoparticles (diameter < 25 nm) of 10 g/L. The table below lists the microhardness and electrical resistance of the Cu, conventional (solid-particle mixing) and sol-enhanced Cu- ZrO_2 composite coatings. The sol-enhanced Cu- ZrO_2 composite coating had a significantly increased microhardness of $\sim 153 \text{ HV}_{50}$ compared to $\sim 133 \text{ HV}_{50}$ of the conventional Cu- ZrO_2 coating.

	Electrical resistance ($\mu\Omega\cdot\text{cm}$)	Microhardness (HV_{50})
Cu	1.76	123
Conventional Cu- ZrO_2	2.92	133
sol-enhanced Cu- ZrO_2	2.33	153

Example 11 - Cu- Al_2O_3 composite coating on carbon steel

[0094] Cu- Al_2O_3 composite coating was prepared by adding Al_2O_3 sol into a conventional electroplating Cu solution. The Al_2O_3 sol was synthesized with Al tri-sec-butoxide ($(\text{C}_2\text{H}_5\text{CH}(\text{CH}_3)\text{O})_3\text{Al}$) as the precursor. A small amount of absolute ethanol was added to 1.7017 g of 97% Al tri-sec-butoxide in a beaker and the increment of mass of 8.0630 g was recorded as the weight of absolute ethanol. The mol ratio of aluminium iso-propoxide and water was 0.01 : 12.4. Under magnetic stirring, 158 mL of de-ionized water was slowly added into the mixture of Al tri-sec-butoxide and ethanol and a few drops of 30% nitric acid were added into the solution to adjust the pH value to 3.5. At this stage, the solution contained white precipitate and it was stirred on a hot plate of 60°C, until all white precipitate dissolved. Finally, a clear aluminium oxide sol was prepared.

[0095] Figure 31 shows the effect of Al_2O_3 sol concentration on the microhardness of coatings. The sol-enhanced Cu- Al_2O_3 coating has a peaking microhardness of $\sim 181 \text{ HV}_{50}$ compared to $\sim 145 \text{ HV}_{50}$ of the Cu coating, indicating $\sim 25\%$ improvement.

REFERENCES CITED IN THE DESCRIPTION

Cited references

This list of references cited by the applicant is for the reader's convenience only. It does not form part of the European patent document. Even though great care has been taken in

compiling the references, errors or omissions cannot be excluded and the EPO disclaims all liability in this regard.

Patent documents cited in the description

- [US5935403A \[0007\]](#)
- [DE4424168 \[0007\]](#)
- [CN101397657 \[0007\]](#)
- [US6183908B \[0007\]](#)
- [JP3253598A \[0007\]](#)
- [US3617363A \[0007\]](#)

PATENTKRAV

1. Fremgangsmåde til plettering eller belægning til fremstilling af en metalkeramisk kompositbelægning på et substrat, **kendetegnet ved** at tilsætte sol af en keramisk fase til pletteringsopløsningen eller -elektrolytten i en mængde, der er kontrolleret til at være tilstrækkelig lav til, at nanopartikler af den keramiske fase dannes direkte på eller ved substratet, hvor molekyler af den keramiske fase eksisterer i en netstruktur i solen, hvor solen tilsættes i et forhold på 0,5 til 100 ml sol pr. liter af pletteringsopløsningen, hvor solen har en koncentration på 20 til 250 gram af den keramiske fase pr. liter af solen, og hvor den keramiske fase er et enkelt eller blandet oxid eller silikat af Ti, W, Si, Zr, Al, Y, Cr, Fe, Pb, Co eller et sjældent jordelement, således at den metalkeramiske belægning dannes på substratet med en overvejende krystallinsk struktur.
- 15 2. Fremgangsmåde til plettering eller belægning ifølge krav 1, der indbefatter tilsætning af solen i en mængde, der er kontrolleret til at undgå dannelse af partikler af den keramiske fase og/eller agglomerering af partikler af den keramiske fase i pletteringsopløsningen eller -elektrolytten.
- 20 3. Fremgangsmåde til plettering eller belægning ifølge krav 1 eller 2, der omfatter tilsætning af solen, mens pletteringen eller belægningen udføres, og med en tilsætningshastighed af solen, der er kontrolleret til at være tilstrækkelig lav til, at nanopartikler af den keramiske fase dannes direkte på eller ved substratet, og/eller at den metalkeramiske belægning dannes på substratet med en overvejende krystallinsk struktur, og/eller at undgå dannelse af nanopartikler af den keramiske fase og/eller agglomerering af partikler af den keramiske fase i pletteringsopløsningen eller -elektrolytten.
- 25 4. Fremgangsmåde til plettering eller belægning ifølge et hvilket som helst af kravene 1 til 3, der omfattet tilsætning af solen i et forhold på 1,25 til 25 ml sol pr. liter af pletteringsopløsningen, hvor solen har en koncentration på 20 til 250 gram af den keramiske fase pr. liter sol.
- 30 5. Fremgangsmåde til plettering eller belægning ifølge et hvilket som helst af kravene 1 til 4, hvor den keramiske fase omfatter TiO_2 , Al_2O_3 eller ZrO_2 .
6. Fremgangsmåde til plettering eller belægning ifølge et hvilket som helst af kravene 1 til 5, hvor belægningen bortset fra den keramiske fase omfatter Ni, Ni-P, Ni-W-P, Ni-Cu-P, Ni-B, Cu, Ag, Au og/eller Pd.

7. Fremgangsmåde til plettering eller belægning ifølge et hvilket som helst af kravene 1 til 6, hvor substratet omfatter stål, Mg, Al, Zn, Sn, Cu, Ti, Ni, Co, Mo, Pb eller en legering deraf.

8. Fremgangsmåde til plettering eller belægning ifølge et hvilket som helst af kravene 5 1 til 7, der er en elektrofri pletterings- eller elektrofri belægningsproces.

9. Fremgangsmåde til plettering eller belægning ifølge krav 8, hvor opløsningen som et reduktionsmiddel omfatter natriumhypophosphit, natriumborhydrid, formaldehyd, dextrose, rochellesalte, glyoxal eller hydrazinsulfat.

10. Fremgangsmåde til plettering eller belægning ifølge et hvilket som helst af kravene 10 1 til 7, der er en galvanisk pletteringsproces.

11. Fremgangsmåde til plettering eller belægning ifølge krav 10, hvor den galvaniske pletteringsproces udføres ved anvendelse af en pletteringsstrøm i området fra 10 mA/cm^2 til 300 mA/cm^2 .

12. Fremgangsmåde til plettering eller belægning ifølge krav 11, hvor den galvaniske 15 pletteringsproces udføres ved anvendelse af en pletteringsstrøm i området fra 20 mA/cm^2 til 100 mA/cm^2 .

DRAWINGS

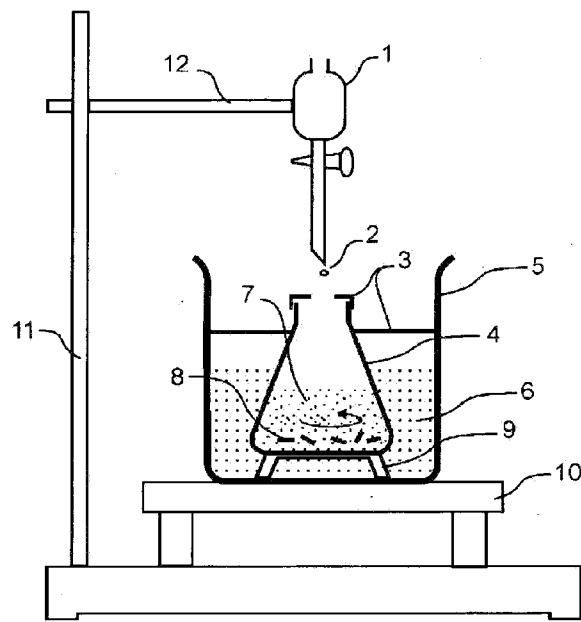


Figure 1

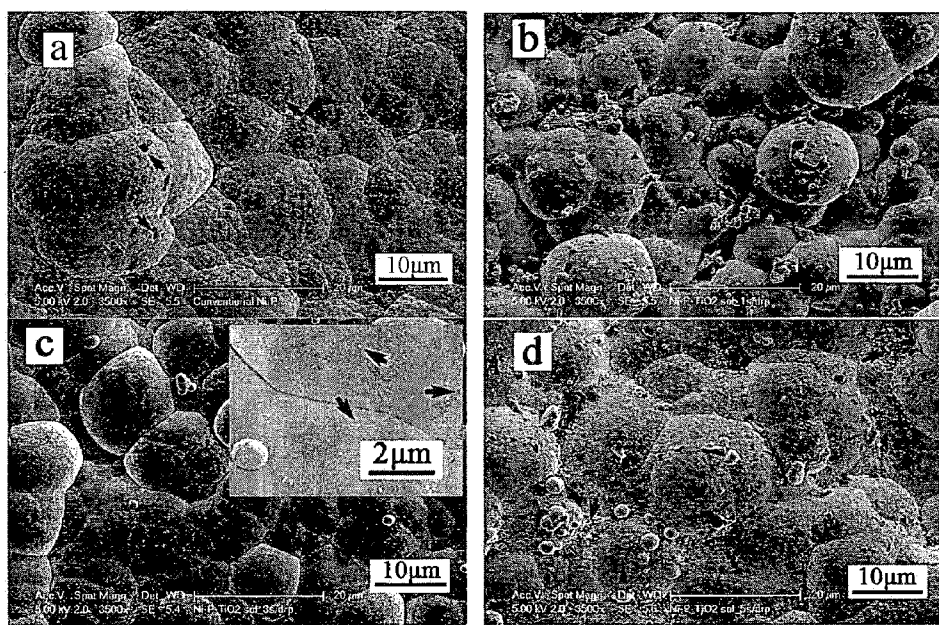


Figure 2

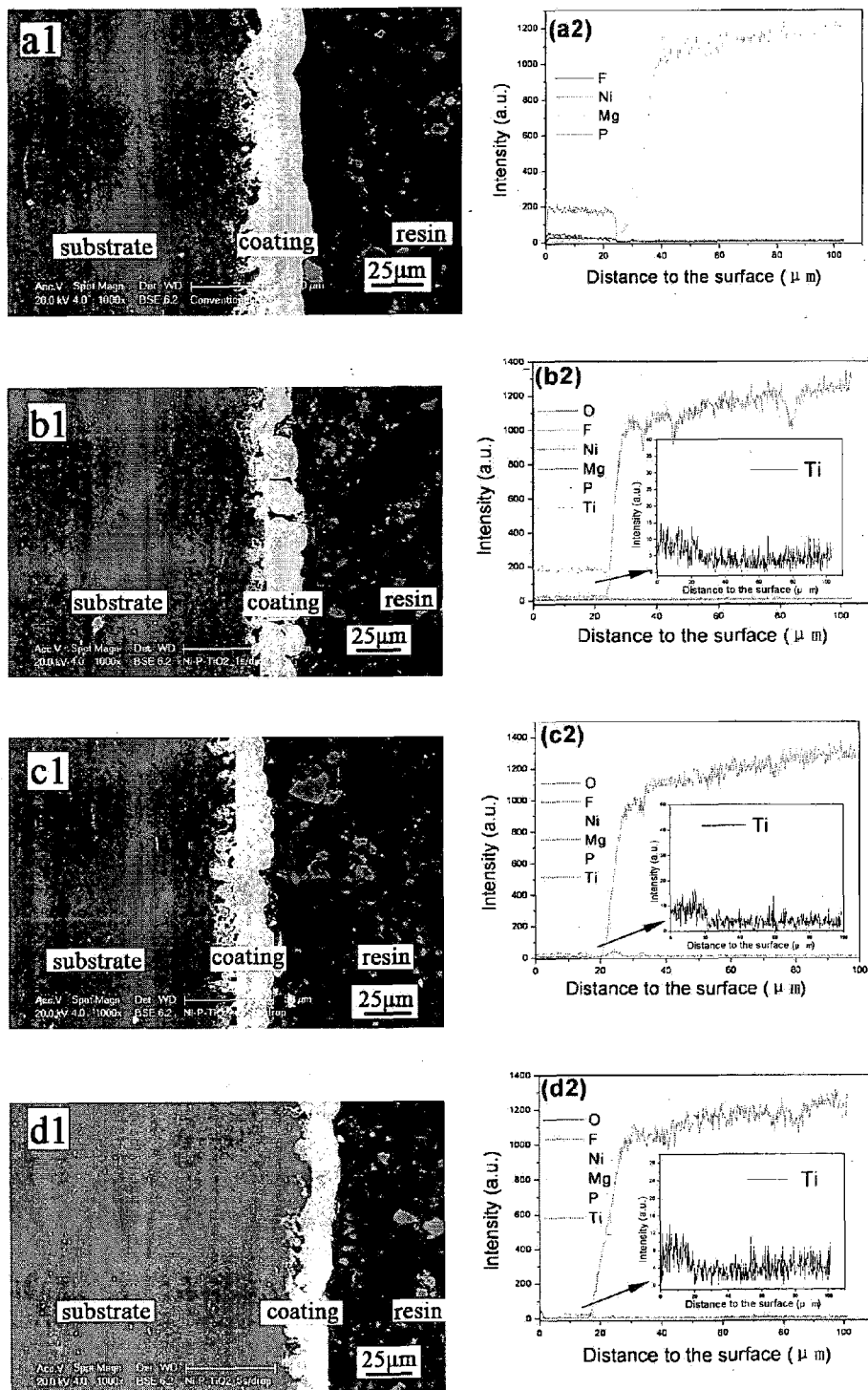


Figure 3

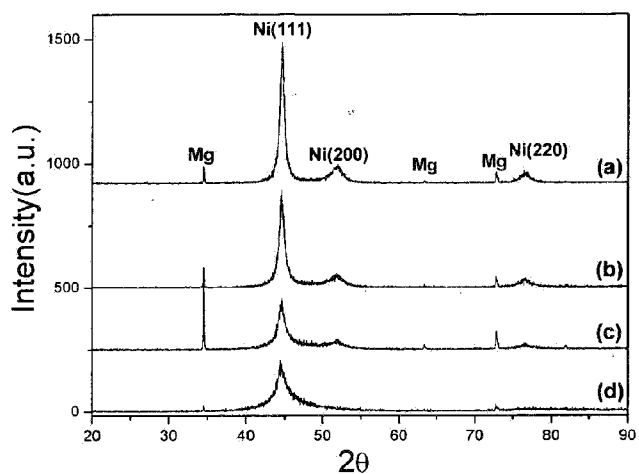


Figure 4

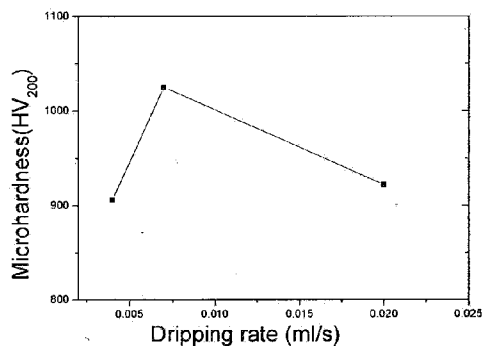


Figure 5

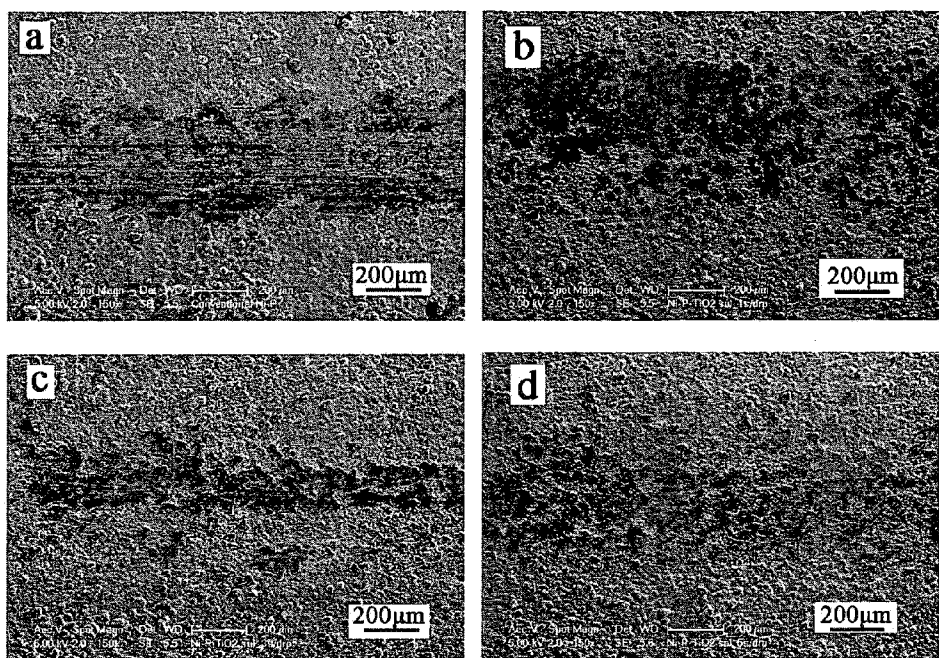


Figure 6

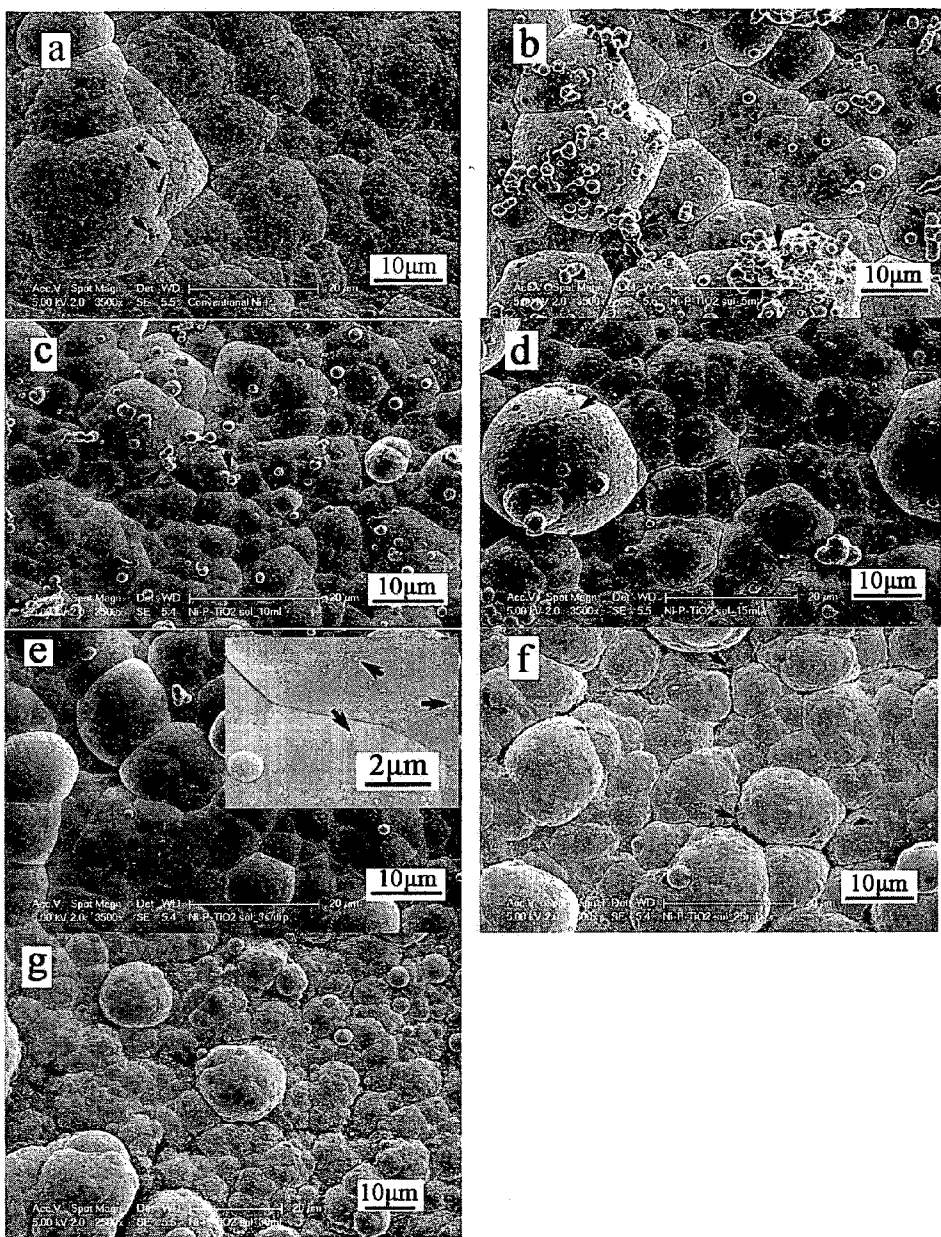


Figure 7

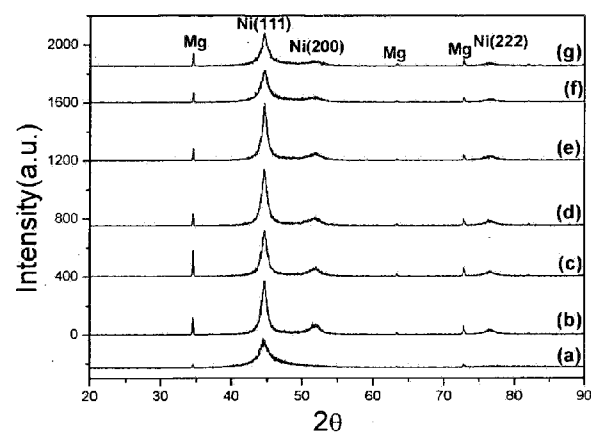


Figure 8

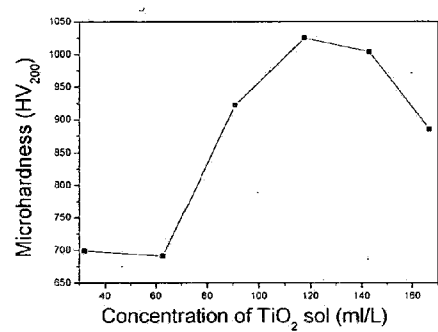


Figure 9

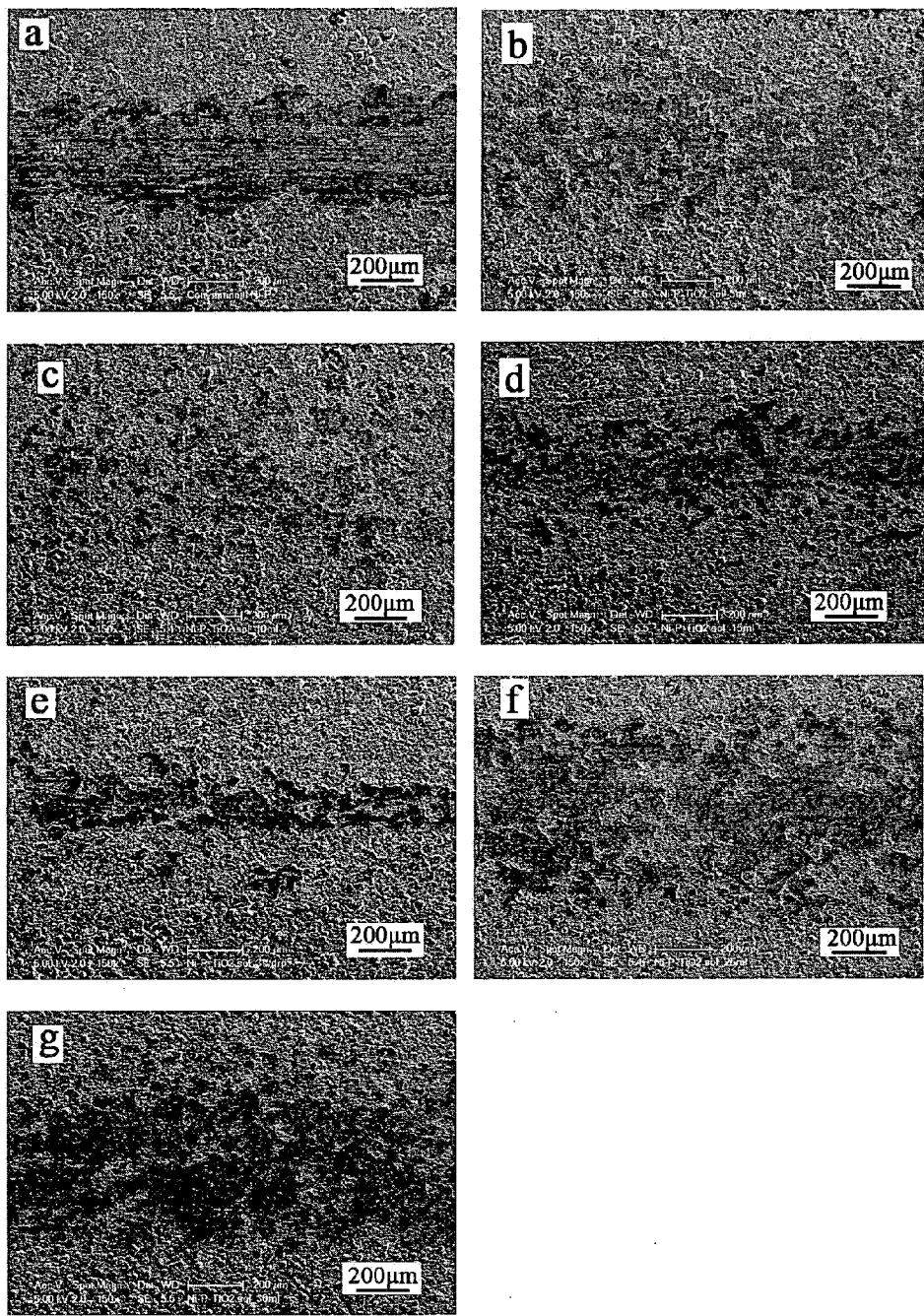


Figure 10

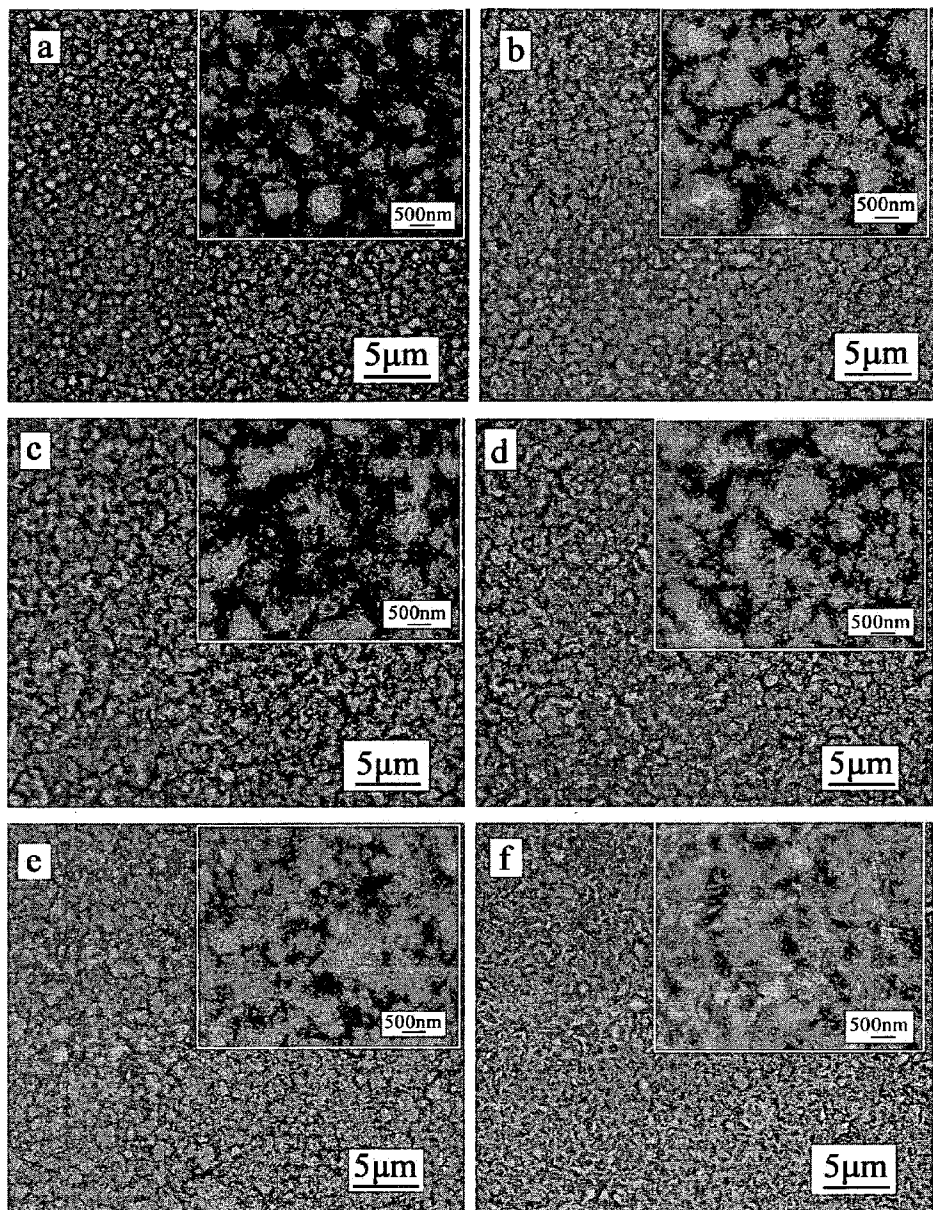


Figure 11

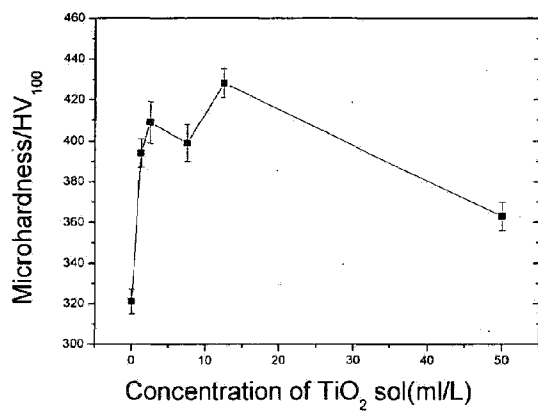


Figure 12

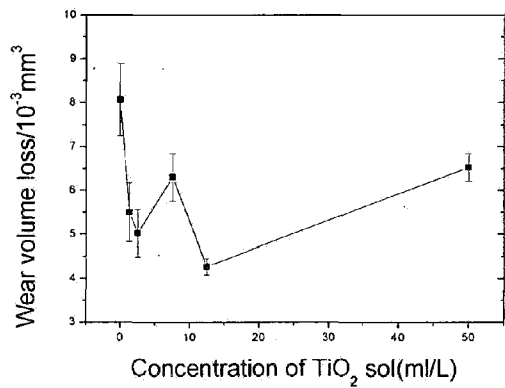


Figure 13

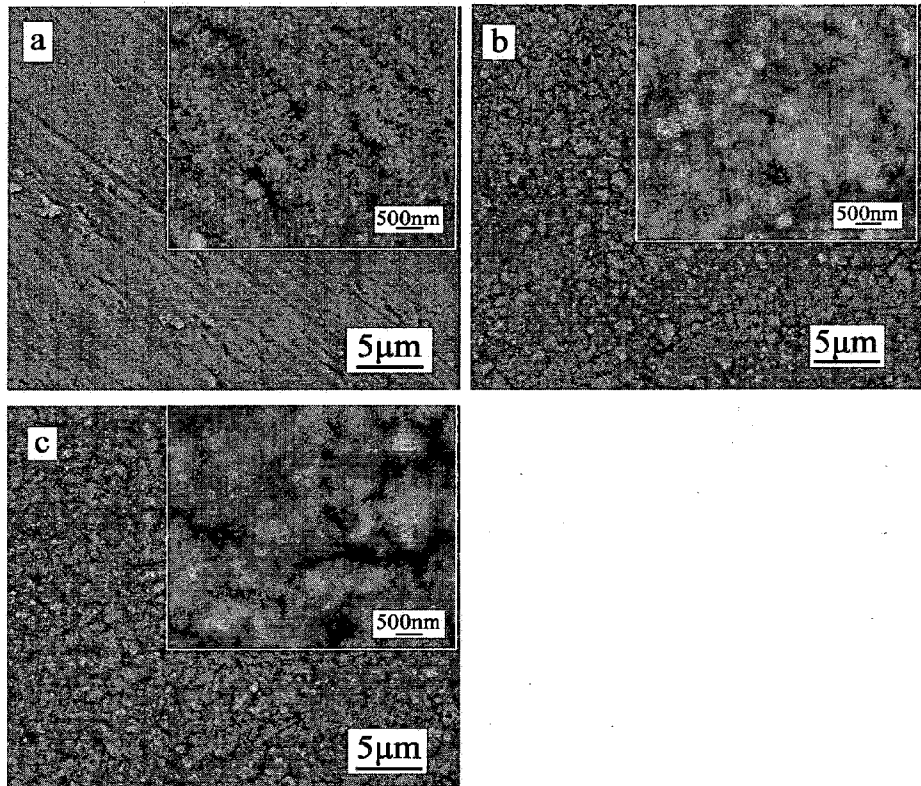


Figure 14

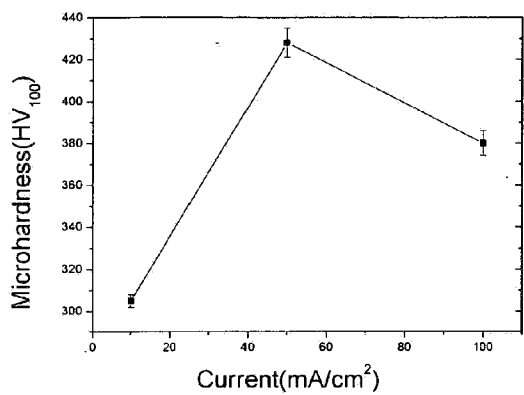


Figure 15

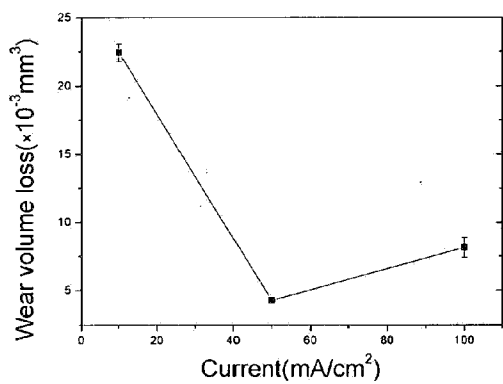


Figure 16

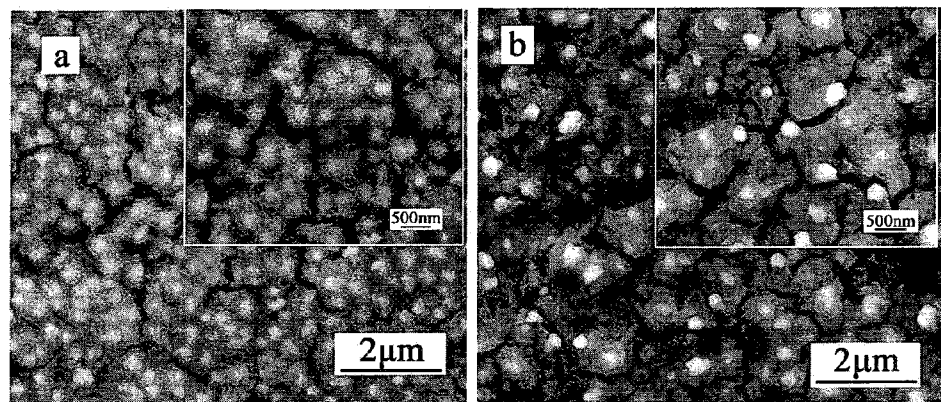


Figure 17

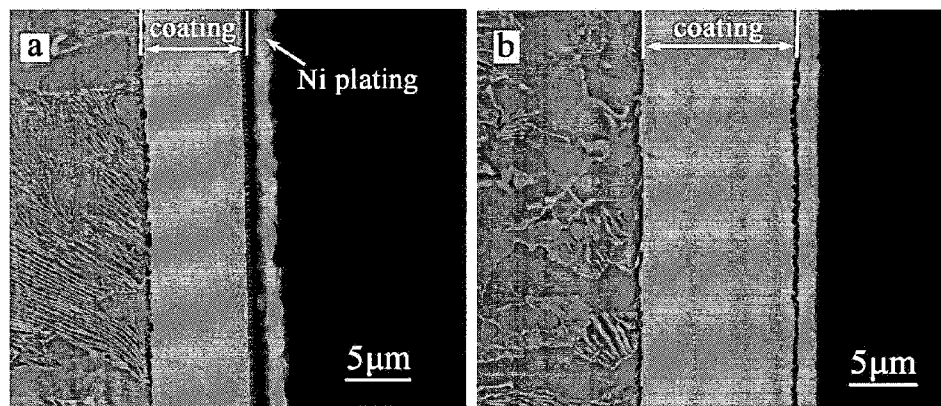


Figure 18

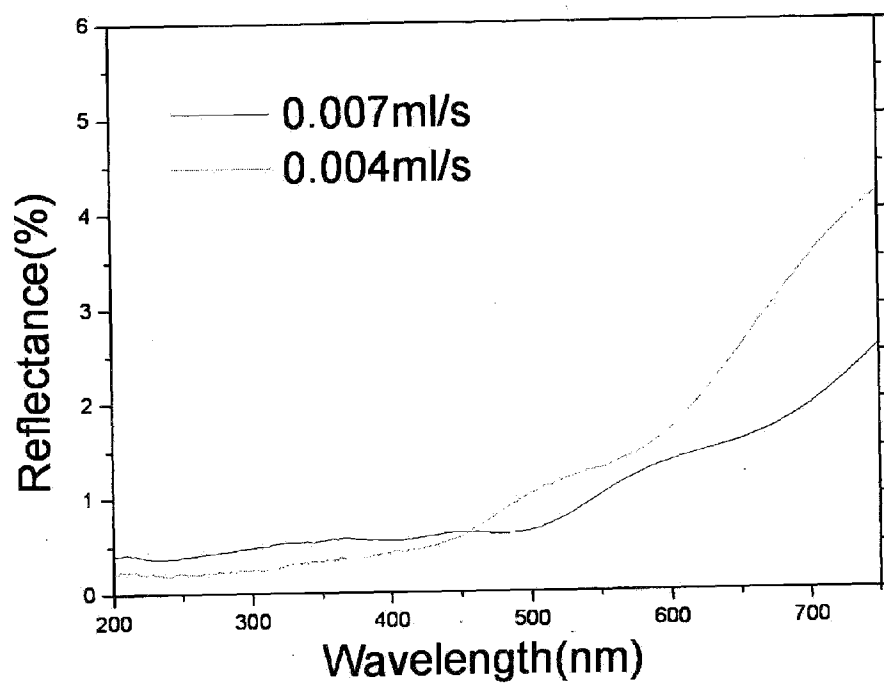


Figure 19

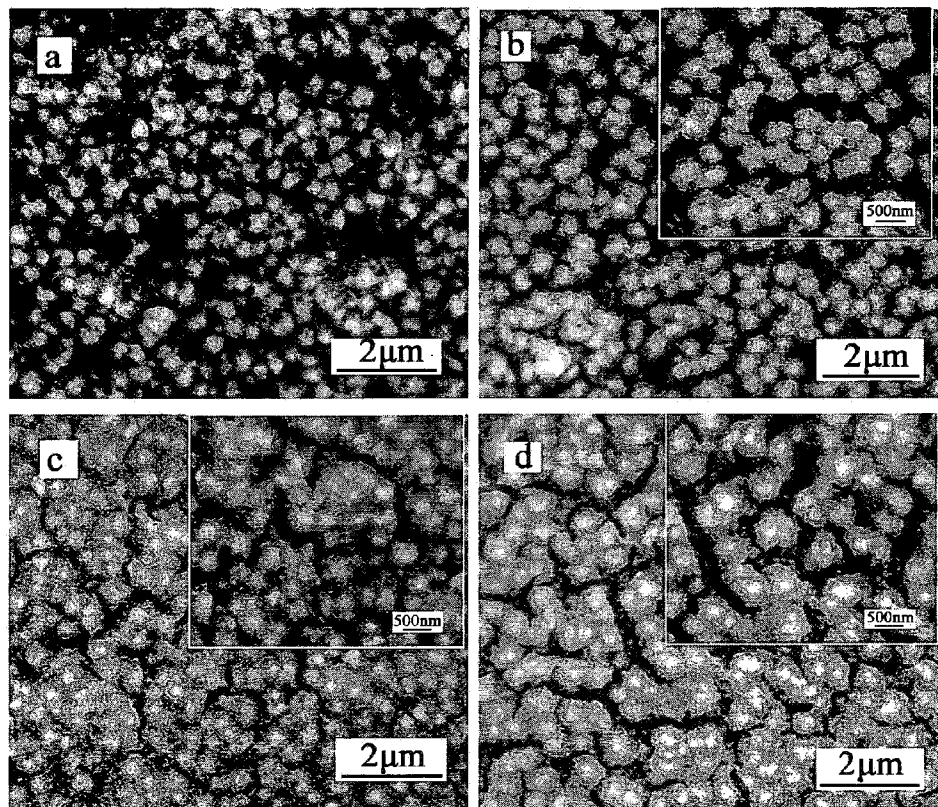


Figure 20

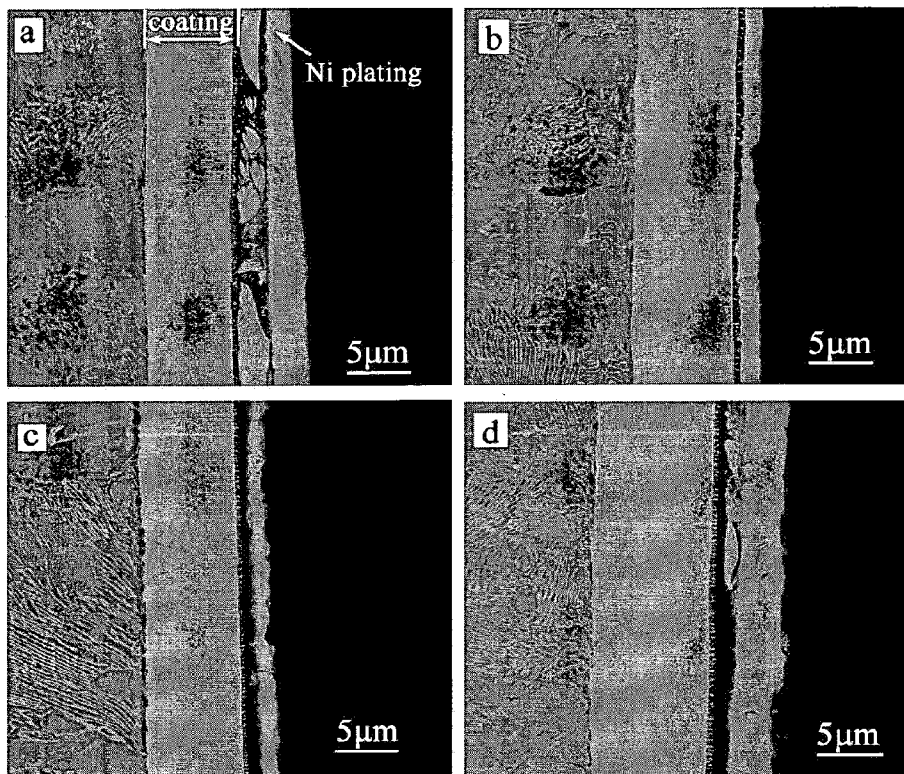


Figure 21

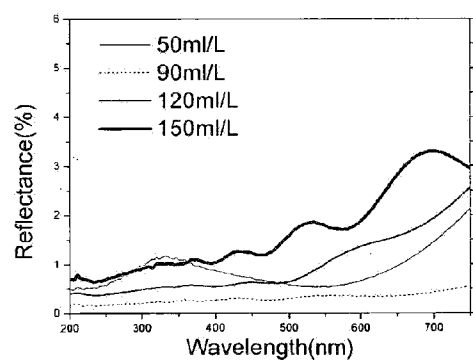


Figure 22

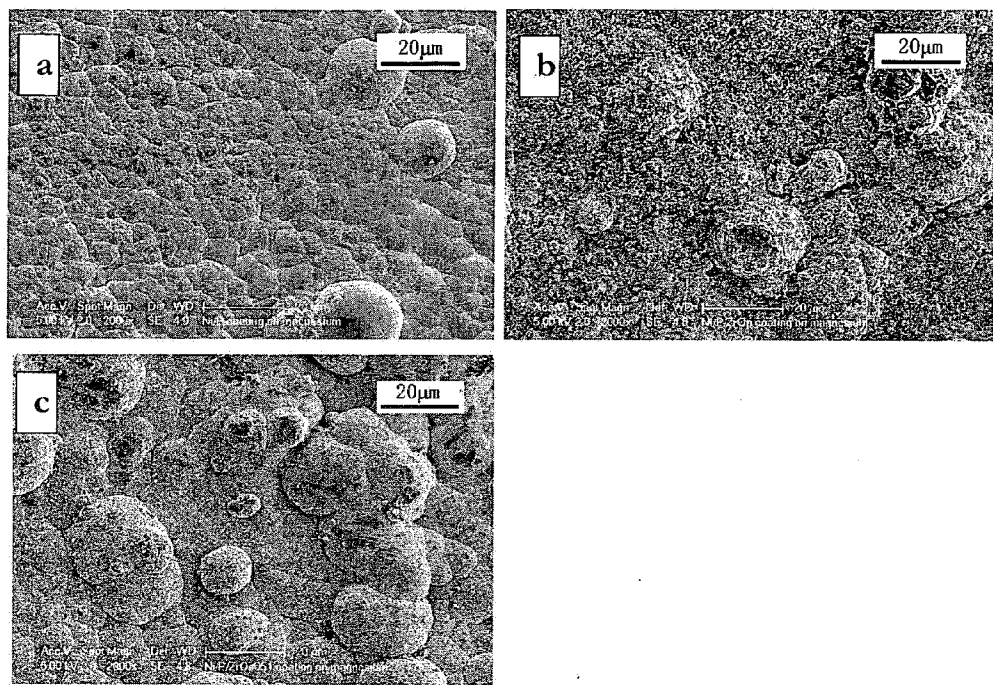


Figure 23

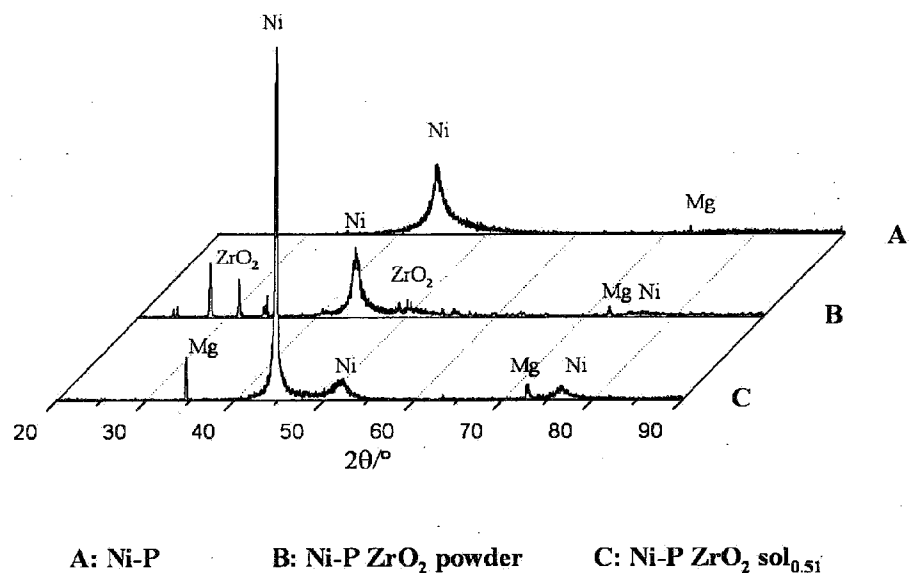


Figure 24

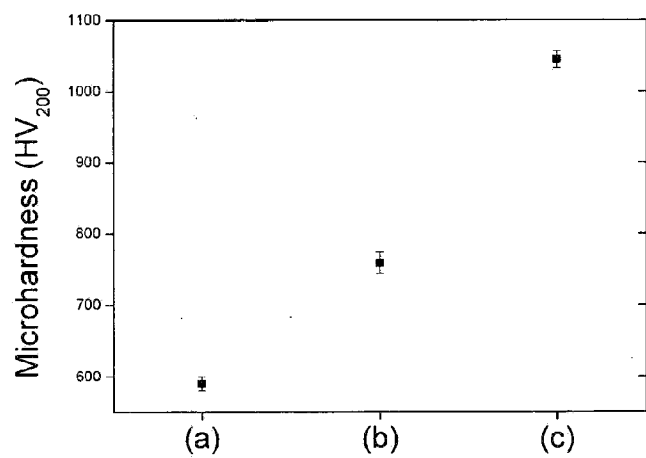


Figure 25

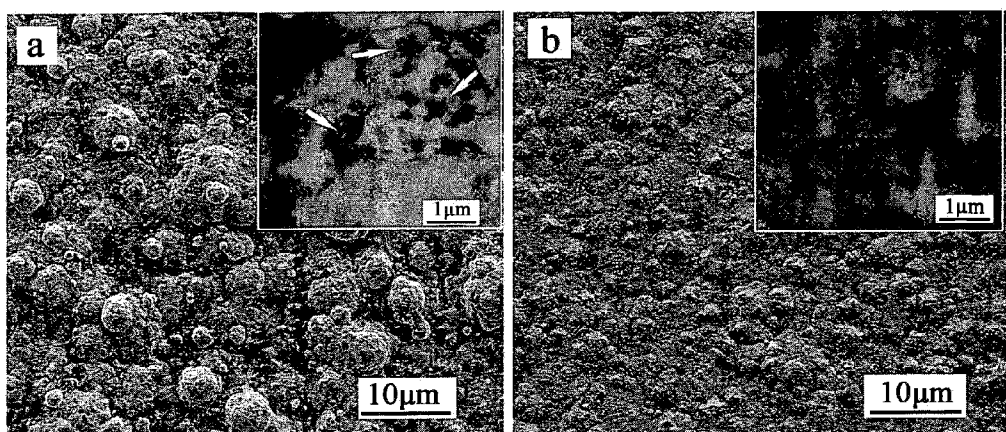


Figure 26

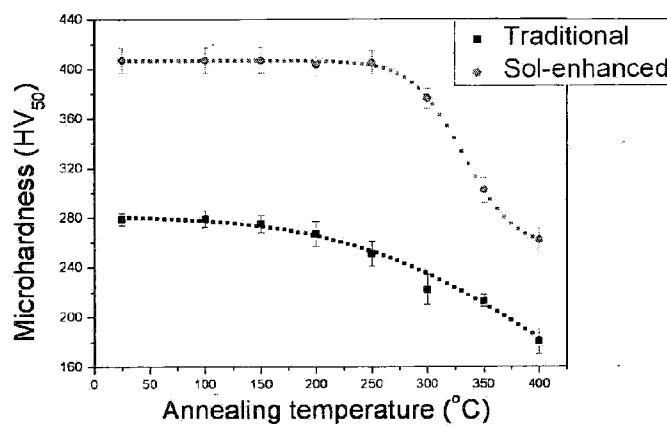


Figure 27

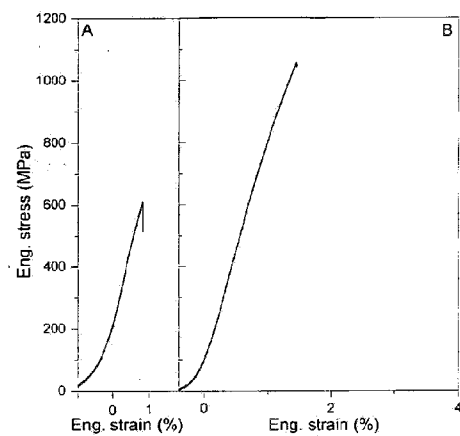


Figure 28

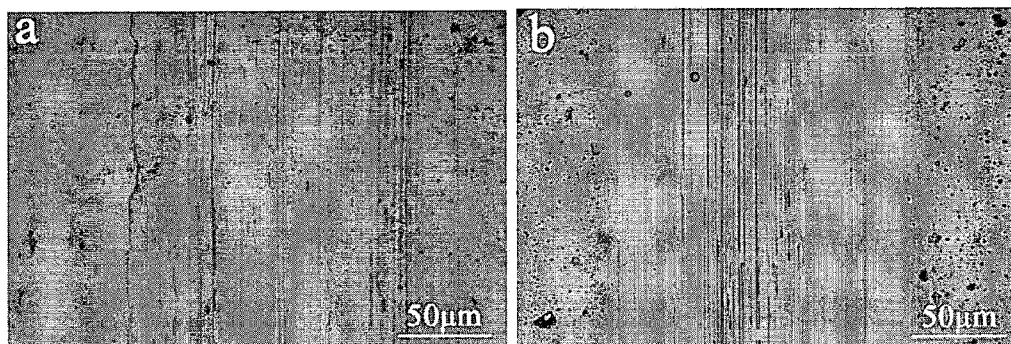


Figure 29

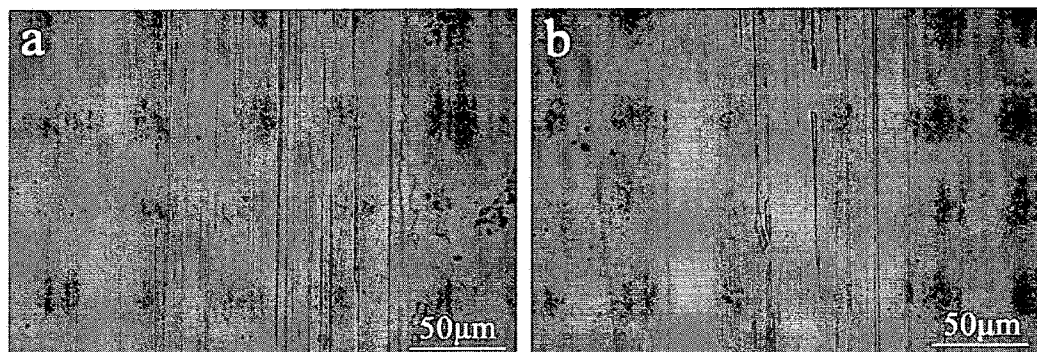


Figure 30

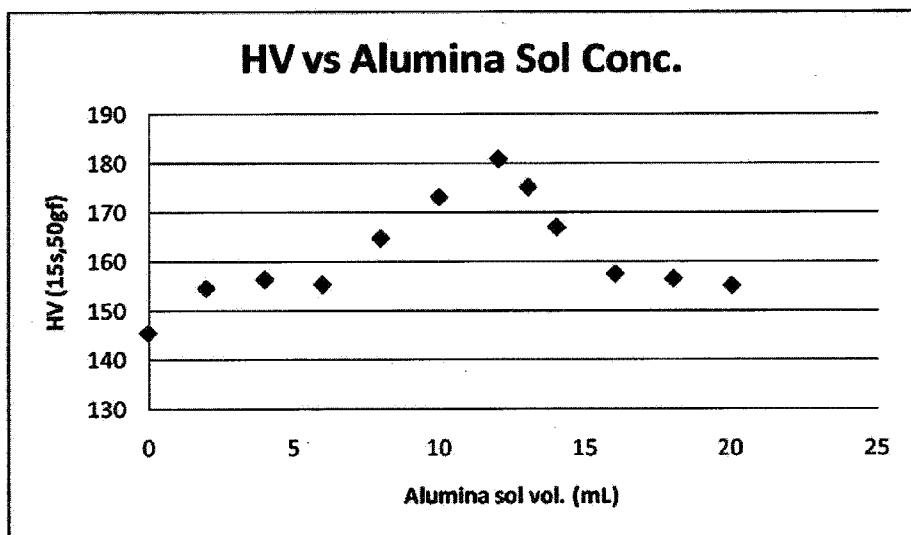


Figure 31